Eur. Phys. J. B **54**, 393–398 (2006)
DOI: 10.1140/epjb/e2007-00001-3

THE EUROPEAN PHYSICAL JOURNAL B

Specific heat spectra for quasiperiodic ladder sequences

D.A. Moreira[1], E.L. Albuquerque[1,2,a], and C.G. Bezerra[1]

[1] Departamento de Física, Universidade Federal do Rio Grande do Norte 59072-970, Natal-RN, Brazil
[2] Center for Polymer Studies and Department of Physics, Boston University 02215-2521, Boston-MA, USA

Received 23 May 2006 / Received in final form 4 September 2006
Published online 5 January 2007 –

Abstract. We performed a theoretical study of the specific heat $C(T)$ as a function of the temperature for double-strand quasiperiodic sequences. To mimic DNA molecules, the sequences are made up from the nucleotides guanine G, adenine A, cytosine C and thymine T, arranged according to the Fibonacci and Rudin-Shapiro quasiperiodic sequences. The energy spectra are calculated using the two-dimensional Schrödinger equation, in a tight-binding approximation, with the on-site energy exhibiting long-range disorder and non-random hopping amplitudes. We compare the specific heat features of these quasiperiodic artificial sequences to the spectra considering a segment of the first sequenced human chromosome 22 (Ch22), a real genomic DNA sequence.

PACS. 82.60.Qr Thermodynamics of nanoparticles – 87.14.Gg DNA, RNA – 87.15.Aa Theory and modeling; computer simulation – 89.75.Da Systems obeying scaling laws

1 Introduction

Recently, we have proposed a single-strand DNA sequence modelling its long and short-range electronic correlations by a quasiperiodic Rudin-Shapiro sequence [1]. An appealing motivation for studying these kind of structures is that they exhibit a highly fragmented energy spectrum displaying a self-similar pattern. From a strictly mathematical perspective, it has been proven that their spectra are *Cantor sets* in the thermodynamic limit [2]. Furthermore, localization of electronic states, one of the most active fields in condensed matter physics, could occur not only in disordered systems but also in the deterministic quasiperiodic systems [3,4]. Another important issue worthy of attention and so far little explored in quasiperiodic structures, is the connection between the scale invariance of their energy spectra and their thermodynamic properties.

The DNA molecule is often described as a one-dimensional random chain, being defined as a sequence of four possible nucleotides which shapes the structure of the amino acids to form proteins. Its sequence can be considered as a symbolic arrangement of a four letter alphabet, namely guanine (G), adenine (A), cytosine (C) and thymine (T), and nothing prevents that the DNA chain can be grown following quasiperiodic sequences as, for instance, the Fibonacci and Rudin-Shapiro ones. Unlike proteins, a π-stacked array of DNA base pairs made up from these nucleotides can provide the way to promote long range charge migration, which in turn gives important clues to mechanisms and biological functions of transport [5].

Simplified fractals based in the Cantor [6,7], as well as the critical attractor of the logistic and circle maps at the onset of chaos [8–10], have been used recently to model the energy spectrum of quasiperiodic systems. The thermodynamic behavior derived from such self-similar spectra display some anomalous features, with the most prominent one being related to the emergence of log-periodic oscillations in the low-temperature behavior of the specific heat. A series of recent works looking for connections with the quasiperiodic aspects of these spectra (scaling laws, fractal dimension, etc.), as well as for some kind of common behavior in the specific heat spectra, have shown, among other things, that the average low-temperature specific heat is intimately connected with some underlying fractal dimension characterizing the energy spectrum [11].

The unique structure of DNA also allows various alterations of its material properties, which could modify its electrical, optical, and thermodynamic properties, revealing additional features. Early theoretical and experimental works on the low-temperature heat capacity of DNA primarily took into account the phonon contributions, specifically the redundant low-energy density of the vibrational states, concluding that the low-energy of the DNA is not unique among biopolymers, and that its specific heat possesses a combination of the properties similar to those of glasses and other disordered materials (see Refs. [12–14] among them). Another important issue concerns the relationship between the low-temperature thermodynamic properties and the multi-fractal character of

[a] e-mail: eudenilson@dfte.ufrn.br

the energy spectra of a sequence dependent double strand DNA molecules. More specifically, what happens to the specific heat spectra profile in these cases? Does it present log-periodic oscillations as a function of the temperature T in the low temperature region, around a mean value given by a characteristic dimension of the energy spectrum? The answers for these and other questions are the main purposes of this paper, which is structured as follows: we present in Section 2 our theoretical model based on an electronic tight-binding Hamiltonian suitable to describe a double-strand of DNA segments with pure diagonal correlated disorder modelled by the quasiperiodic chain of Fibonacci (FB) and Rudin-Shapiro (RS) type. For comparison, we have also calculated the electronic energy spectra of the first sequenced human chromosome 22 (Ch22), a real genomic DNA sequence. Section 3 deals with the specific heat profiles associated to the electronic energy spectra described in Section 2. Finally, the conclusions of this work are summarized in Section 4.

2 Energy spectra

Our Hamiltonian is an effective tight-binding model describing one electron moving in a ladder geometry, composed by two interconnected chains of sites, side by side, with a single orbital per site and nearest-neighbor interactions (see Fig. 1). The corresponding time dependent Schrödinger equation is given by ($\hbar = 1$):

$$\begin{aligned} t(\psi_{n+1}^{\alpha} + \psi_{n-1}^{\alpha}) + w\psi_n^{\beta} &= (E - \epsilon_n^{\alpha})\psi_n^{\alpha}, \\ t(\psi_{n+1}^{\beta} + \psi_{n-1}^{\beta}) + w\psi_n^{\alpha} &= (E - \epsilon_n^{\beta})\psi_n^{\beta}. \end{aligned} \tag{1}$$

Here ϵ_n^{α} is the single energy at the orbital ψ_n^{α} (the upper index refers to the chain, while the lower index refers to the site position in each chain). Also t and w are the intra-chain and the inter-chain first-neighbor electronic overlaps (hopping amplitude), respectively.

Within this framework, the (discrete) Schrödinger equation can be written as

$$\begin{pmatrix} \psi_{n+1}^{\alpha} \\ \psi_{n+1}^{\beta} \\ \psi_n^{\alpha} \\ \psi_n^{\beta} \end{pmatrix} = M(n) \begin{pmatrix} \psi_n^{\alpha} \\ \psi_n^{\beta} \\ \psi_{n-1}^{\alpha} \\ \psi_{n-1}^{\beta} \end{pmatrix}, \tag{2}$$

where $M(n)$ is the transfer matrix

$$M(n) = \begin{pmatrix} (E - \epsilon_n^{\alpha})/t & -w/t & -1 & 0 \\ -w/t & (E - \epsilon_n^{\beta})/t & 0 & -1 \\ 1 & 0 & 0 & 0 \\ 0 & 1 & 0 & 0 \end{pmatrix}. \tag{3}$$

After successive applications of the transfer matrix $M(n)$, we have

$$\begin{pmatrix} \psi_{n+1}^{\alpha} \\ \psi_{n+1}^{\beta} \\ \psi_n^{\alpha} \\ \psi_n^{\beta} \end{pmatrix} = M(n)M(n-1)\cdots M(2)M(1) \begin{pmatrix} \psi_1^{\alpha} \\ \psi_1^{\beta} \\ \psi_0^{\alpha} \\ \psi_0^{\beta} \end{pmatrix}. \tag{4}$$

In this way we have the wave function at arbitrary site. Calculating this product of transfer matrices is completely equivalent to solve the Schrödinger equation for the system.

Defining the ket formed by the the orbitals of the Nth unitary cell, i.e.:

$$|\psi^{(N)}\rangle = \begin{pmatrix} \psi_{N+1}^{\alpha} \\ \psi_{N+1}^{\beta} \\ \psi_N^{\alpha} \\ \psi_N^{\beta} \end{pmatrix}, \tag{5}$$

and taking into account that in our model, each generated sequence is an unitary cell whose repetition builds up the entire DNA molecule, Bloch's ansatz for each chain yields:

$$|\psi^{(N+1)}\rangle = T|\psi^{(N)}\rangle = \exp(iQ_iL)|\psi^{(N)}\rangle, \tag{6}$$

with Q_i being Bloch's wavevector and L the periodic distance. Therefore,

$$[T - \exp(iQ_iL)I]|\psi^{(N)}\rangle = 0, \tag{7}$$

where I is the identity matrix. Since T is an unimodular matrix ($\det T = 1$), its eigenvalue should satisfy $\lambda_1\lambda_2\lambda_3\lambda_4 = 1$, i.e., $\lambda_2 = \lambda_1^{-1}$ and $\lambda_4 = \lambda_3^{-1}$, implying the existence of only two independent eigenvalues. Therefore Bloch's wavevector should satisfy

$$\exp(iQ_rL) = \lambda_r, \;\; r = 1, 2. \tag{8}$$

The secular equation is then:

$$\lambda^4 + \Xi\lambda^3 + \Gamma\lambda^2 + \Xi\lambda + 1 = 0, \tag{9}$$

where $\Xi = -Tr[T]$ (Tr meaning the trace of the matrix T) and

$$\begin{aligned} \Gamma = (T_{11} + T_{22})(T_{33} + T_{44}) - T_{34}T_{43} - T_{12}T_{21} - T_{13}T_{31} \\ - T_{14}T_{41} - T_{23}T_{32} - T_{24}T_{42} + T_{11}T_{22} + T_{33}T_{44}. \end{aligned} \tag{10}$$

Here T_{ij} are the elements of the matrix T. Rearranging equation (9), we have:

$$\gamma^2 + \Xi\gamma + \Gamma - 2 = 0. \tag{11}$$

Here $\gamma_i = (\lambda_i + \lambda_i^{-1})$, are the roots of the second-order degree equation, each one corresponding to one of the independent eigenvalues of the matrix T. Its explicit form is:

$$\gamma_{1,2} = \frac{-\Xi \pm \sqrt{\Xi^2 - 4(\Gamma - 2)}}{2}. \tag{12}$$

For the DNA sequence of the first sequenced human chromosome 22 (Ch22), entitled NT_{011520}, the numbers of letters of this sequence is about 3.4×10^6 nucleotides. This sequence was retrieved from the internet page of the National Center of Biotechnology Information. The energies ϵ_n are chosen from the ionization potential of the respective bases [15], i.e., $\epsilon_A = 8.24$, $\epsilon_T = 9.14$, $\epsilon_C = 8.87$, and

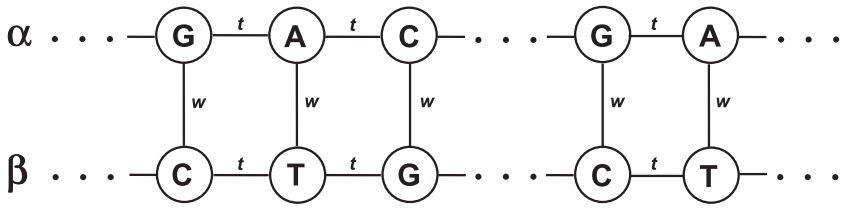

Fig. 1. Schematic representation of a double-strand DNA molecule, showing the intra-chain (t) and the inter-chain (w) first-neighbor hopping terms.

$\epsilon_G = 7.75$, all units in eV, representing the adenine, guanine, thymine, and cytosine molecules, respectively. The hopping term t among the bases were taken equal to 1 eV, since theoretical calculations using ab initio methods yield for this potential values in the range 0.4–1 eV [16,17]. The hopping potential w due to the hydrogen bonds linking the two strands is considered to be 0.1 eV.

The quasiperiodic Fibonacci sequence belongs to the family of the so-called substitutional sequences, which are characterized by the nature of their Fourier spectrum. It exhibits a dense pure point Fourier measure, characteristic of a true quasicrystal-like structure (for a review of the physical properties of these and others quasiperiodic structures see Ref. [18]). It can be constructed starting from a G (guanine) nucleotide as seed and following the inflation rule $G \to GC$, $C \to G$. The sequence produced by this method is then utilized to fill one line in our matrix representative of DNA (see Fig. 1); the other one is filled according to the complemental base pairs rules: $A-T$ and $G-C$.

On the other hand, the quasiperiodic Rudin-Shapiro structure, which belongs also to the family of the so-called substitutional sequences, displays an absolutely continuous Fourier measure, a property which it shares with the random sequences [19]. Starting, as in the Fibonacci case, from a G (guanine) nucleotide as seed, it can be built through the inflation rules $G \to GC$, $C \to GA$, $A \to TC$, and $T \to TA$, using also the same complemental base pairs rules $A-T$ and $G-C$, as in the Fibonacci case.

In all structures above described modelling the DNA molecule, the presence of long range correlations avoids canonical approaches like perturbation theory, where one first separates a small localized piece of the system, treating the rest as perturbation a posteriori. This approach does not work in our cases, because the behavior of the macroscopic system is completely distinct of the behavior of its separated small piece, due to the long range correlations. Fortunately, the presence of long range correlations itself gives the key to circumvent this difficulty: normally these systems are very robust to wide modifications on a microscopic scale. The important consequence of this robustness, i.e., many systems which are distinct within a microscopic scale presenting the same critical behavior, is that one can thus classify the various systems in a few universality classes. Further, it is worthy to mention here that the finite sampling sizes we will consider in the following study of the thermodynamics properties are large enough to achieve the scaling behavior of the multifractal spectrum.

With the intention of comparing these quasiperiodic sequences with the genomic one, we assume also that the energies ϵ_n take the values ϵ_G, ϵ_A, ϵ_C, and ϵ_T, as in the DNA genomic sequence, with the same numerical values.

Figure 2 shows the electron energy spectra, as measured by their equivalent bandwidth Δ (the sum of all allowed energy regions in the band structures), for the Fibonacci (Fig. 2a) and the Rudin-Shapiro (Fig. 2b) quasiperiodic sequences, as well as for the genomic DNA (Fig. 2c), respectively, up to the number of nucleotides n equal to 93. This is nothing but the Lebesgue measure of the energy spectrum. From there, one can infer the forbidden and allowed energies as a function of the number of nucleotides n. Notice that, as expected, as n increases the allowed band regions get narrower and narrower, as an indication of more localized modes. We have also investigate their multifractal behavior which is, in general, a common property of strange attractors in nonlinear systems [20]. In order to characterize these objects, it is convenient to introduce the function $f(\alpha)$, known as the *multifractal spectrum* or the *spectrum of scaling indices*. Loosely, one may think of the multifractal as an interwoven set of fractals of different dimensions $f(\alpha)$, where α is a measure of their relative strength [21]. The formalism relies on the fact that highly nonuniform probability distributions arise from the nonuniformity of the system. Usually, the singularity spectrum has a parabolic-like shape, distributed in a finite range $[\alpha_{min}, \alpha_{max}]$, which are the minimum and maximum singularity strengths of the intensity measure, respectively. They correspond also to the exponents governing the scaling behavior in the most concentrated and rarefied regions of the attractor. The value of the $\Delta\alpha = \alpha_{max} - \alpha_{min}$ may be used as a parameter to measure the degree of randomness of the band width distribution. Summarizing, we found:

(a) for the quasiperiodic Fibonacci sequence, we have $\alpha_{min} = 0.835$ and $\alpha_{max} = 1.858$ ($\Delta\alpha = 1.023$);
(b) for the quasiperiodic Rudin Shapiro sequence, we have $\alpha_{min} = 0.743$ and $\alpha_{max} = 3.821$ ($\Delta\alpha = 3.078$);
(c) for the human chromosome 22 (Ch22) DNA chain, we have $\alpha_{min} = 0.414$ and $\alpha_{max} = 3.612$ ($\Delta\alpha = 3.198$).

From the above, we can infer that regarding the degree of randomness of the band width distribution for each structure, the RS sequence is more close related to the Ch22 structure than the FB one.

We now turn to the specific heat's calculation, considering the above described energy spectra, which is the topic of the next section.

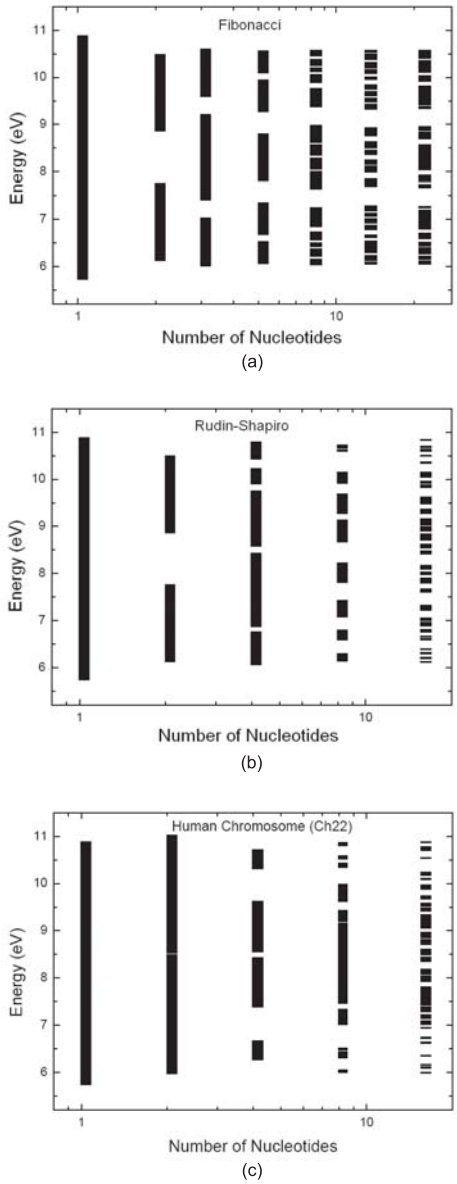

Fig. 2. Energy spectra for (a) Fibonacci DNA chain; (b) Rudin-Shapiro DNA chain; (c) human chromosome 22 (Ch22) DNA chain.

3 Specific heat spectra

We address now the specific heat obtained from the spectra shown in Figure 2. The description below, which follows the lines of reference [22], is general and has been successfully applied to many other banded spectra. In Figure 2 each spectrum, for a fixed number of nucleotides n, has m allowed continuous bands. We consider the level density within each band to be constant. The partition function for n nucleotides spectrum, using a Maxwell-Boltzmann statistics is given by

$$Z_n = \int_0^\infty \rho(\epsilon) e^{-\beta\epsilon} d\epsilon. \tag{13}$$

Here $\beta = 1/T$ (by choosing the Boltzmann's constant $k_B = 1$), and we take the density of states $\rho(\epsilon) = 1$. We justify the use of a classical Maxwell-Boltzmann statistics because for fermions, as it was already discussed [23,24], the classical scenario survives the inclusion of a more appropriate quantum Fermi-Dirac statistics. Besides, the specific heat in this regime does not vanishes at low temperatures but instead oscillates log-periodically, whose pattern is the main focus of this work.

After a straightforward calculation we can write Z_n as

$$Z_n = \frac{1}{\beta} \sum_{i=1,3,\ldots}^{2m-1} e^{-\beta\epsilon_i}[1 - e^{-\beta\Delta_i}]. \tag{14}$$

Here the subscript n is related with the number of nucleotides, m is the number of allowed bands, and $\Delta_i = \epsilon_{i+1} - \epsilon_i$ is the difference between the top and bottom energy levels of each band. The specific heat is then given by

$$C_n(T) = \frac{\partial}{\partial T}\left[T^2 \frac{\partial \ln Z_n}{\partial T}\right], \tag{15}$$

which can be written as

$$C_n(T) = 1 + \frac{\beta f_n}{Z_n} - \frac{g_n^2}{Z_n^2}. \tag{16}$$

Here

$$f_n = \sum_{i=1,3,\ldots}^{2m-1} [\epsilon_i^2 e^{-\beta\epsilon_i} - \epsilon_{i+1}^2 e^{-\beta\epsilon_{i+1}}], \tag{17}$$

and

$$g_n = \sum_{i=1,3,\ldots}^{2m-1} [\epsilon_i e^{-\beta\epsilon_i} - \epsilon_{i+1} e^{-\beta\epsilon_{i+1}}]. \tag{18}$$

Therefore, once we know the electronic energy spectra of a given DNA chain, we can determine the associated specific heat by using (16).

Figure 3a shows the electronic specific heat spectra for the Fibonacci DNA chains, corresponding to its 10th (number of nucleotides $n = 89$), 11th (number of nucleotides $n = 144$), 12th (number of nucleotides $n = 233$), and 13th (number of nucleotides $n = 377$) generation numbers, as a function of the temperature. For the high-temperature limit ($T \to \infty$), the specific heat for all cases converges and decays as T^{-2}. This is a consequence of the existence of a maximum energy value in the spectrum (once the spectrum is bounded). As the temperature decreases, the specific heat increases up to a maximum value. The corresponding temperature for this maximum value depends on the number of nucleotides n, although one can see a clear tendency for a common temperature value as n increases. After the maximum value, the specific heat falls into the low temperature region. In this region it starts to present a non-harmonic small oscillation behavior, as shown in the inset of Figure 3a. This can be interpreted as a superposition of Schottky anomalies corresponding to the scales of the energy spectrum. Furthermore, the profiles of these oscillations define clearly two classes of

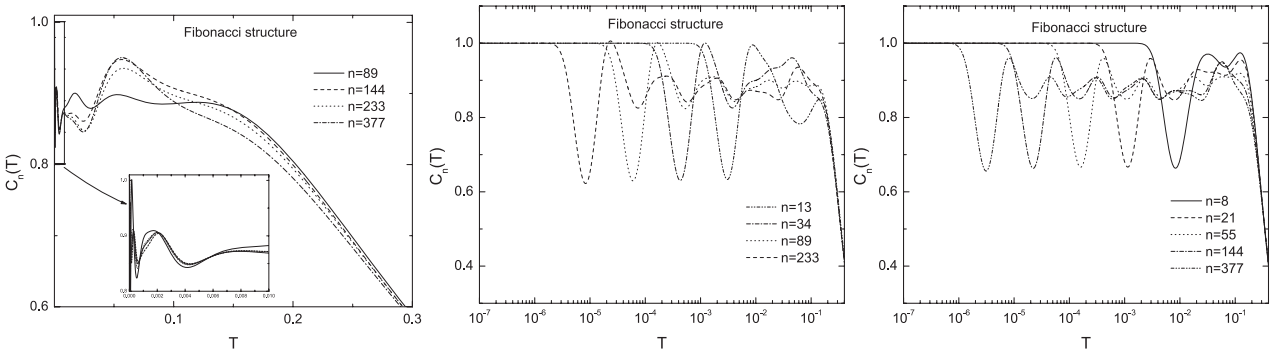

Fig. 3. (a) Specific heat (in units of k_B) versus temperature (in units of Δ, the sum of all allowed energy regions in the band structures) for the Fibonacci DNA chain. The inset shows the low-temperature behavior of the specific heat. (b) Log-periodic behavior of the specific heat for the even (6th, 8th, 10th, and 12th generation, respectively) Fibonacci DNA chain. (c) Log-periodic behavior of the specific heat for the odd (5th, 7th, 9th, 11th, and 13th generation, respectively) Fibonacci DNA chain.

oscillations, as far as the parity (even or odd) of the generation number of the Fibonacci sequence is concern, with the amplitude of the even oscillations being bigger than the amplitude of the odd ones. These behaviors are better illustrated in Figures 3b and 3c, where are depicted log-plots of the specific heat against the temperature, showing clearly a log-periodic behavior, i.e., $C_n(T) = AC_n(aT)$, where A is a constant, and a an arbitrary number. The mean value d, around it $C(T)$ oscillates log-periodically, can be given approximately by the so-called spectral dimension (the exponent of a power law fit of the integrated density of states), associated to the minimum singularity exponent α in the multifractal curve $f(\alpha)$, namely $\alpha_{min} = 0.835$. Of course, the number of oscillations observed in the specific heat spectra is related to the number of nucleotides n, once n depends on the hierarchical generation of the Fibonacci sequence (more oscillations appear as n increases).

A different scenario appears when one consider the other quasiperiodic structure studied here (i.e., modelling the DNA molecule by the RS sequence), which is depicted in Figure 4. Similarly to the Fibonacci case, in the limit when $T \to \infty$, the specific heat goes to zero as T^{-2} for all values of n. Also there are oscillations in the region near to $T \to 0$ (which are better shown by the inset of the figure). Although these oscillations can be interpreted as Schottky anomalies, as in the Fibonacci case, they do not have the same standard of behavior, i.e., two groups of oscillations corresponding to even and odd generation numbers of the sequence. Additional differences should be pointed out. In this case there are oscillations with amplitude very superior to those found in the Fibonacci case. More important, the log-plot does not show a log-periodic behavior. Instead, it shows an erratic-like profile, which can be attributed to the more disordered structure of the Rudin-Shapiro sequence. Therefore, apart of the common asymptotic behavior of the specific heat when $T \to \infty$ and $T \to 0$, there is no other connection between the Fibonacci and Rudin-Shapiro DNA chains considered here, regarding their specific heat spectra.

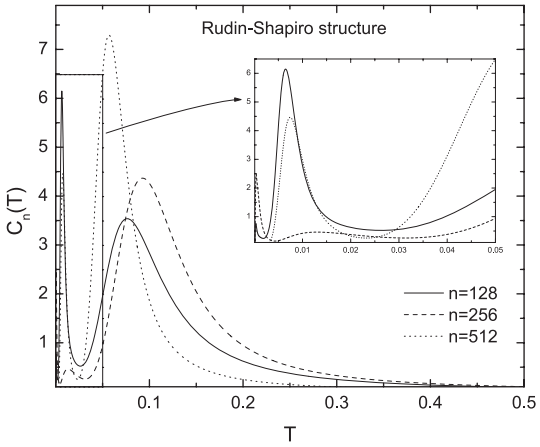

Fig. 4. Specific heat (in units of k_B) versus temperature (in units of Δ, the sum of all allowed energy regions in the band structures) for the Rudin-Shapiro DNA chain, corresponding to its 8th (number of nucleotides $n = 128$), 9th (number of nucleotides $n = 256$), and 10th (number of nucleotides $n = 512$) generation number. The inset shows the low-temperature behavior of the specific heat.

Finally, for comparison purposes, we present in Figure 5 the specific heat behavior of the human chromosome Ch22 chain. As in the two previous cases, in the limit when $T \to \infty$, the specific heat goes to zero as T^{-2} and also there are oscillations in the low temperature region due to Schottky anomalies (which are better shown by the inset of the figure). One can see clearly that the overall behavior of the specific heat of Ch22 DNA chains is very close to the specific heat of the Rudin-Shapiro one, in contrast with the Fibonacci case. For example, Ch22 and Rudin-Shapiro specific heats both present similar amplitude of oscillations, as well as an erratic-like behavior in their log-plots, instead of the log-periodic behavior found in the Fibonacci case.

Before concluding, let us comment on a possible connection between the present work with those of Mrevlishvili and collaborators [13,14]. Their experimental results show oscillations of the specific heat at low

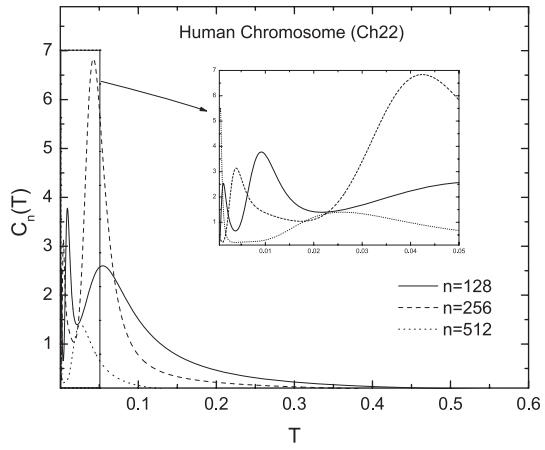

Fig. 5. Specific heat (in units of k_B) versus temperature (in units of Δ, the sum of all allowed energy regions in the band structures) for the Ch22 DNA chain, corresponding to the number of nucleotides $n = 128$, 256, and 512. The inset shows the low-temperature behavior of the specific heat.

temperature, which are qualitatively similar to our present numerical theoretical results. They attribute their results to the non-crystalline order of the DNA samples which may be modelled, as we have shown in this article, by quasiperiodic systems.

4 Conclusions

In summary, we have studied the thermodynamical properties of long-range correlated double strand DNA molecules. More specifically, we have performed a theoretical study of the electronic specific heat behavior of DNA chains modelled by the quasiperiodic Fibonacci and Rudin-Shapiro sequences, aiming to further contribute to the present understanding of the role played by correlations on the electronic properties of DNA segments.

Our numerical results show that the specific heat for all cases, in the high-temperature limit ($T \to \infty$), converges and decays as T^{-2} (once the spectra are bounded). Other general feature of these systems is the oscillatory behavior of the specific heat in the low temperature regime. However, the low temperature behavior strongly depends on the sequence applied in the construction of the system. For the Fibonacci DNA chains there is a parity even-odd of the specific heat oscillations, while for the Rudin-Shapiro one, no parity emerges from the specific heat oscillations. Besides, a well defined log-periodicity was found for the Fibonacci specific heat profile, while an erratic log-plot behavior is the main signature of the Rudin-Shapiro case. In order to unreveal the actual relevance of long range correlations, which is a kind of signature of the quasiperiodic sequences, we compared the specific heat spectra considering segments of the Ch22 human chromosome with those resulting from the quasiperiodic sequences, with a remarkable agreement with the Rudin-Shapiro one.

We would like to thank partial financial support from the Brazilian Research Agencies CNPq-Edital Universal, CNPq-Rede Nanobioestruturas and FINEP-CTInfra. One of us (ELA) also thanks a Capes-Fulbright scholarship at the Center for Polymer Studies, Boston University, in Boston-MA, USA.

References

1. E.L. Albuquerque, M.S. Vasconcelos, M.L. Lyra, F.A.B.F. de Moura, Phys. Rev. E **71**, 21910 (2005)
2. A. Bovier, J.-M. Ghez, Commun. Math. Phys. **158**, 45 (1993)
3. J.B. Sokoloff, Phys. Rep. **126**, 189 (1985)
4. E.L. Albuquerque, M.G. Cottam, Phys. Rep. **376**, 225 (2003)
5. S. Roche, Phys. Rev. Lett. **91**, 108101 (2003)
6. C. Tsallis, L.R. da Silva, R.S. Mendes, R.O. Vallejos, A.M. Mariz, Phys. Rev. E **56**, R4922 (1997)
7. P. Carpena, A.V Coronado, P. B-Galván, Phys. Rev. E **61**, 2281 (2000)
8. H.-O. Peitgen, H. Jurgens, D. Saupe, *Chaos and Fractals* (Springer-Verlag, Heidelberg, 1992)
9. L.R. da Silva, R.O. Vallejos, C. Tsallis, R.S. Mendes, S. Roux, Phys. Rev. E **64**, 11104 (2001)
10. I.N. de Oliveira, M.L. Lyra, E.L. Albuquerque, L.R. da Silva, J. Phys.: Condens. Matter **17**, 3499 (2005)
11. P.W. Mauriz, E.L. Albuquerque, M.S. Vasconcelos, Phys. Rev. B **63**, 184203-6 (2001)
12. I.-S. Yang, A.C. Anderson, Phys. Rev. B **35**, 9305 (1987)
13. G.M. Mrevlishvili, L.L. Buishvili, G. Sh. Japaridze, G.R. Kakabadze, Thermochimica Acta **290**, 65 (1996)
14. G.M. Mrevlishvili, Thermochimica Acta **308**, 49 (1998)
15. H. Sugiyama, I. Saito, J. Am. Chem. Soc. **118**, 7063 (1996)
16. A.A. Voityuk et al., J. Chem. Phys. **114**, 5614 (2001)
17. H. Zhang et al., J. Chem. Phys. **117**, 4578 (2002)
18. E.L. Albuquerque, M.G. Cottam, *Polaritons in Periodic and Quasiperiodic Structures* (Elsevier, Amsterdam, 2004)
19. F. Axel, J.P. Allouche, Z.Y. Wen, J. Phys. Condens. Matter **4**, 8713 (1992)
20. I. Procaccia, in *Proceedings of Nobel Symposium on Chaos and Related Problems*, Phys. Scr. **T9**, 40 (1985)
21. T.C. Halsey, P. Meakin, I. Procaccia, Phys. Rev. Lett. **56**, 854 (1986)
22. C.G. Bezerra, E.L. Albuquerque, A.M. Mariz, L.R. da Silva, C. Tsallis, Physica A **294**, 415 (2001)
23. R.O. Vallejos, C. Anteneodo, Phys. Rev. E **58**, 4134 (1998)
24. I.N. de Oliveira, M.L. Lyra, E.L. Albuquerque, Physica A **343**, 424 (2004)